Renewable Energy 167 (2021) 652–661

Contents lists available at ScienceDirect

Renewable Energy

journal homepage: www.elsevier.com/locate/renene

Biomass CO_2 gasification with CaO looping for syngas production in a fixed-bed reactor

Ningbo Gao [a, **], Maciej Śliz [b, *], Cui Quan [a], Artur Bieniek [b], Aneta Magdziarz [b]

[a] School of Energy and Power Engineering, Xi'an Jiaotong University, Xi'an, 710049, China
[b] AGH, University of Science and Technology, 30 Mickiewicza Av., 30-059, Kraków, Poland

ARTICLE INFO

Article history:
Received 6 May 2020
Received in revised form
27 October 2020
Accepted 24 November 2020
Available online 29 November 2020

Keywords:
gasification
CO_2 capture
CaO looping
TG-FTIR

ABSTRACT

The most important challenge in solid feedstock thermal conversion methods is minimising CO_2 emissions. In this work, the gasification of pine sawdust in a mixture of N_2 and CO_2 was investigated for the reduction of CO_2 by a calcium oxide loop. The experiments were conducted at 600, 700, and 800 °C in a fixed-bed reactor. The biomass was mixed with the calcium oxide at a ratio of 1:1. The chemical composition of the syngas was analysed using gas chromatography. Moreover, the high heating values of the received gas samples were calculated, and thermogravimetric analysis and Fourier-transform infrared spectroscopy analysis were performed to investigate the absorption of CO_2 by CaO. The results of the gasification process showed that the syngas contained CO, CH_4, CO_2, H_2, N_2, and other low hydrocarbons. The most significant results were obtained for a 2:1 ratio of N_2 to CO_2 at 700 °C, and a CO_2 reduction of 25% was observed. Moreover, the catalytic properties of CaO increased the concentration of H_2 in the produced syngas by up to 10%. A temperature of 800 °C was too high for the carbonation reaction of CaO. This study presents a possible solution for achieving negative carbon emissions.

1. Introduction

The increasing demand for primary energy and the depletion of fossil fuel resources are major problems in the current energy sector. The International Energy Agency regularly reports on the annual global primary energy supply; global primary energy demand in 2007 was approximately 139 872 TWh (12 029 Mtoe). By 2017, demand had increased to 162 465 TWh (13 972 Mtoe), 81.3% of which was developed from fossil fuels and 18.7% from other energy sources, such as biofuels, nuclear, or renewable (solar, wind) [1,2]. Thus, the global energy sector is largely based on fossil fuels with restricted resources.

The greenhouse gases (especially carbon dioxide, the primary product of man-made fossil fuel combustion) emitted during the conversion of chemical energy from fossil fuels to other kinds of energy increase the surface temperature of the Earth and have a huge impact on climate change. According to international agreements, CO_2 emissions will be restricted by 50–80% by 2050 [3,4].

Environmental protection and the continuity of primary energy production are the primary reasons for researching alternative energy sources that decrease the consumption of fossil fuels. One such source is biomass, defined by the United Nations Framework Convention on Climate Change as biodegradable organic material originating from plants, animals, microorganisms, and municipal solid wastes [5].

Raw biomass is characterised by high moisture content, low calorific value, and high molar ratios of O/C and H/C [6]. These properties are the reason why raw biomass causes operating problems during the combustion process. The energy potential of raw biomass can be increased by upgrading its properties by subjecting to pre-treatment processes, such as torrefaction, hydrothermal carbonisation, pyrolysis, or gasification [7–12]. The thermal conversion process is defined as a transformation of solid feedstock (in this case, biomass) into products with a higher energy potential. These processes produce solid, liquid, and gaseous products, such as charcoal, tar, and syngas. The efficiency and concentration of each phase depend on the technology used.

Biomass gasification is a high-temperature decomposition process of biomass in the presence of a gasification agent, such as steam, air, or oxygen, into gaseous products that can be used in the energy sector and in chemical technology [13]. Gasification involves processes, such as the drying of raw biomass and pyrolysis, that

* Corresponding author.
** Corresponding author.
E-mail addresses: nbogao@xjtu.edu.cn (N. Gao), msliz@agh.edu.pl (M. Śliz).

https://doi.org/10.1016/j.renene.2020.11.134

release tar vapour and non-condensable gases and convert biomass particles into biochar. The overall gasification process is as follows:

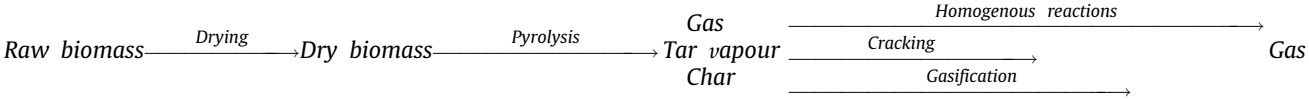

During gasification, the heavy hydrocarbons bonds of tar vapours are broken due to thermal cracking and tar is converted into low-molecular-weight gases. At the same stage, the biochar and non-condensable gases involve several reactions with a gasification agent. Equations (1)–(4) show reactions between solid biochar and typical gasification medium [14,15].

$$char + O_2 \rightarrow CO_2 + CO \quad (1)$$

$$char + CO_2 \rightarrow CO \quad (2)$$

$$char + H_2O \rightarrow CH_4 + CO \quad (3)$$

$$char + H_2 \rightarrow CH_4 \quad (4)$$

Low-molecular-weight gases are produced during the homogeneous reaction between gasifying agents and non-condensable gases created during pyrolysis or thermal cracking. Some of the reactions are known by popular names, such as oxidation, shift reaction, methanation, and steam-reforming reactions.

Gasification is highly efficient, has a small influence on the natural environment, and indirectly contributes CO_2 emissions reduction [16]. The primary advantage of gasification is the high amount of gases in the products—especially syngas, in steam gasification. Syngas is a mixture of carbon monoxide and hydrogen. The production of hydrogen has grown rapidly owing to the high demand for new technologies. Hydrogen is used in power plants and catalytically converted (with carbon monoxide) into other chemical compounds by the Fischer–Tropsch method [17].

Recent studies have investigated the use of carbon dioxide as a gasifying agent. This process leads to some benefits, such as the possibility of recycling CO_2 and decreasing green gas emissions [18,19]. Carbon dioxide as a gasifying agent can maximise the production of low-molecular-weight gases by the Boudard reaction and allows the removal of heavy hydrocarbons (tars) from bio-oil vapours [20,21]. Although CO_2 has favourable gasification process properties, its high concentration in the products of the thermal conversion processes is not desirable [22]. The concentration of CO_2—considered the principal greenhouse gas—in the natural environment has a large impact on climate change. Therefore, carbon dioxide emissions have been restricted by international agreements [23,24].

Many investigations have proposed methods to decrease CO_2 production in gasification processes based on chemical solutions [25–30]. Chemical methods, the most conventional, include two techniques of carbon dioxide capture from biomass gasification—which can offer high efficiency. The first method is calcium looping, which provides a low concentration of carbon dioxide in the gaseous products of gasification [31]. The second method is chemical absorption via monoethanolamine [32]. Calcium looping technology, which promises low cost due to common access to CaO, adds calcium oxide to a line with the gaseous products of biomass gasification or directly to the reactor bed with raw biomass. Due to the CaO content, a heterogonous and exothermic reaction between carbon dioxide and calcium oxide occurs and can be expressed by equation (5):

$$\boldsymbol{CaO + CO_2 \rightarrow CaCO_3 + 177.8 kJ/mol} \quad (5)$$

The addition of calcium oxide has a few important aspects that can improve the efficiency of the thermal conversion process of solid fuel. The primary function of the described process is the absorption and removal of CO_2 from the gasification products [33–35]. Furthermore, CaO sorbent can enhance hydrogen production [36–38] and methane reformation [39,40]. Carbon dioxide removal shifts thermochemical equilibrium and leads to the production of gases with higher energy potential, such as methane and hydrogen. In addition to CO_2 capture, the introduced calcium oxide and its reaction with carbon dioxide is a heat source that may partially cover the energy demand in endothermic gasification.

In recent years, there has been rising interest in the gasification process connected with CaO looping, primarily to produce enriched syngas during biomass gasification by removing carbon dioxide. Wu et al. and others have tried to obtain a higher calorific value for the obtained gas by increasing hydrogen and carbon monoxide yields and decreasing carbon dioxide content [41–46]. Nam et al. investigated the effect of calcium oxide on tar removal [47]. Nevertheless, calcium oxide is most commonly used because of its catalytic properties and the possibility of the in-situ capture of carbon dioxide. Investigation of the connection between CaO looping and gasification in a carbon dioxide atmosphere also attracts interest. Chein et al. modelled this process by investigating different ratios of CaO to C [48]. Zhang et al. experimentally investigated gasification under a CO_2 atmosphere in the presence of CaO, but focused on small amounts of CO_2 in the gasifying atmosphere [49]. Another study by Sun and Wu was conducted at 650 °C [50]. To the best of the authors' knowledge, opportunity for research on this topic remains. This paper presents experimental investigations of the impact of the presence of calcium oxide on carbon dioxide capture during pine sawdust gasification in a fixed-bed reactor with a mixture of nitrogen and carbon dioxide as gasification agents. The primary aim of this study was to investigate the effect of temperature and CO_2 concentration in the gasifying atmosphere on gas production and their amount and calorific value. The use of calcium oxide was aimed at enhancing hydrogen production, supplying additional energy for the gasification reaction, and decreasing the CO_2 content in the final product. We emphasise that the gasification of such biomass in a CO_2 atmosphere has not been widely studied. Herein, a possible solution for achieving a process with negative carbon emissions is presented.

2. Materials and methods

2.1. Material

Pine sawdust (PSD) was used as a biomass feedstock for this

investigation. PSD from a sawmill in Xianyang, Shaanxi, China was dried, milled, and collected between a 60–100 mesh, which yielded particles of sizes of 0.14–0.23 mm. Proximate analysis of pine sawdust showed typical values for biomass. High volatile matter content (82.03%) and low ash, and moisture content (1.29% and 2.77%, respectively) were determined. The calculated fixed carbon was 13.91%. Calcium oxide (CaO) was used as an absorber of CO_2. CaO was specially prepared by preheating up to 900 °C to ensure its purity (without moisture content). During the experiments, nitrogen (N_2) and carbon dioxide (CO_2) gases were used to ensure a gasification atmosphere.

2.2. Gasification experiments

Gasification was conducted in a fixed-bed reactor (Fig. 1) produced by the Longkou Yuanbang Electric Furnace Manufacturing Company, China. The principal element of the setup was a vertical glass tube (50 cm in length and 3 cm in diameter). The reactor was heated by an electric furnace equipped with a 1 kW heater. The bed was set on a permeable barrier 20 cm from the bottom end of the tube. First, quartz wool was put in to secure samples from falling. Next, 3 g of biomass was thoroughly mixed with 3 g of calcium oxide. Subsequently, another layer of quartz wool was installed. After mixing, the gases went through the bed and reacted to the flask in an ice bath where tar was condensed. The gas analyser required dry samples; thus, the next element was a water vapour absorber with silica gel. Gases were collected in Tedlar bags. To determine the influence of temperature and composition of the gasifying atmosphere, the temperature of the furnace and the gas flow rate were controlled. Tests were conducted at 600 °C, 700 °C, and 800 °C with flow rates equal 30 ml/min for nitrogen and carbon dioxide. The concentration of CO_2 in the gasifying agent 50%. At 700 °C, the test was conducted without the addition of calcium oxide with the same flow rates of N_2 and CO_2. Further tests with CaO at 700 °C were performed using different flow rates to achieve specific N_2:CO_2 ratios. 60 mL/min N_2 and 0 ml of CO_2 produced a ratio of 1:0 (0% CO_2); 40 ml/min of N_2 and 20 ml/min of CO_2 produced a 2:1 ratio (33% CO_2); and 20 ml/min of N_2 and 40 mL/min of CO_2 produced a 1:2 ratio (67% of CO_2). The parameters of the gasification experiments are summarised in Table 1.

Table 1
Experimental parameters.

Test number	0	1	2	3	4	5	6
Gasification temperature, °C	700	600	700	700	700	700	800
Mass of pine sawdust, g	3	3	3	3	3	3	3
Mass of calcium oxide, g	3	3	0	3	3	3	3
Ratio of N_2:CO_2 flow rates	1:0	1:1	1:1	1:1	2:1	1:2	1:1

2.3. Analytical methods

Ultimate analysis of biomass and char samples was performed using an Elemental Truspec Analyser LECO CHN628 that determines the carbon, nitrogen, and hydrogen content in organic matter using a combustion method. An encapsulated and preweighed sample was introduced to the furnace with pure oxygen and combusted to carbon dioxide (CO_2) and steam (H_2O). NO_x is simultaneously created due to the high reaction temperature. High temperatures allow for the oxidation of investigated elements and further distinction via infrared and thermal conductivity detectors.

Gas chromatography analysis was used to analyse the chemical composition of gas and conducted with a GC7900, Tianmei Scientific Instrument Company, China. The chromatograph was equipped with a flame ionisation detector and a thermal conductivity detector. Ar was used as the carrier gas. During each gasification experiment, gas was collected to two Tedlar bags. The first sample was collected during the heating stage of the reactor from 300 to 700 °C (and from 200 to 600 °C for gasification conducted at 600 °C). The second bag was collected in final conditions at the desired temperature. Every bag was filled for exactly 20 min. Later, based on known nitrogen flow rate and peaks area from gas chromatography, the volume of other gas components was calculated.

Thermogravimetric analysis (TGA) was conducted using a DTG-60M/IR-1S instrument (Shimadzu, Japan). Samples receiving CaO were heated from 20 to 900 °C at a heating rate of 20 °C/min and maintained at 900 °C for 30 min. The analysis was conducted in a nitrogen atmosphere with a flow rate of 75 mL/min. Mass, time, and temperature were measured to plot thermogravimetric (TG), derivative of thermogravimetric (DTG), and differential thermal analysis (DTA) curves.

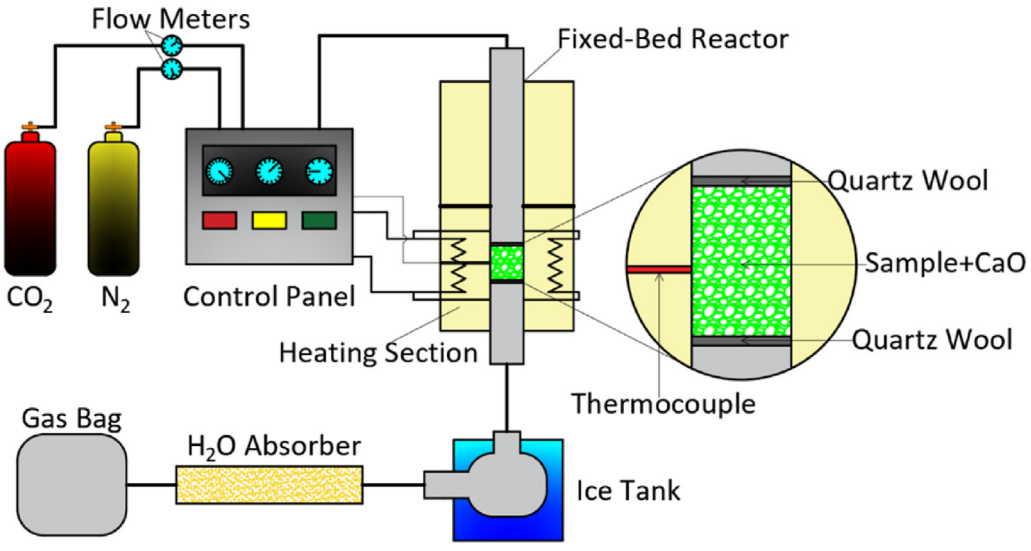

Fig. 1. A scheme of gasification setup.

Fourier-transform infrared spectroscopy (FTIR) analysis connected to TGA was performed for the chosen sample (700 °C, PSD + CaO, 1:1 N_2:CO_2) in a Nicolet 6700 Flex, Thermo Fisher Scientific. The sample was heated to 900 °C at a heating rate of 20 °C/min in a nitrogen atmosphere (75 mL/min). Every minute, a portion of the gas was analysed by infrared spectroscopy.

The high heating value (HHV) of the obtained syngas was calculated using tabular values for each component [51]. The results of this study allowed us to compare potential usefulness as fuel.

3. Results and discussion

Analyses of chars and syngas allowed the determination of the influence of temperature, gasifying atmosphere, and addition of calcium oxide on hydrogen and carbon dioxide production. The results are presented below in suitable sections.

3.1. Ultimate analysis

Ultimate analysis allowed the observation of the carbonisation of raw biomass under gasification conditions without the addition of calcium oxide (2nd test). The carbon content increased from 47.3% for raw biomass to 84.5% for char after gasification at 700 °C. The hydrogen content simultaneously decreased from 6.45 to 2.25%. The results for other samples were misleading due to mixed calcium oxide and calcium carbonate in the chars.

3.2. Thermogravimetric analysis

The amount carbon dioxide absorbed by calcium oxide was calculated based on a thermogravimetric analysis of obtained chars mixed with CaO conducted in a nitrogen atmosphere. Results are presented in Figs. 2 and 3. The visible mass loss is attributed to the decomposition of $CaCO_3$ and the reaction between released CO_2 and biochars. To compare different gasification conditions, the entire detected mass loss was to correspond to the mass of released CO_2 [52–54]. The mass of released CO_2 was converted to the volume with the assumption that 1 mol of CO_2 weighs 44 g and takes up 22.42 dm^3 at standard temperature and pressure. The mass of the residue after the gasification experiment (mixture of biochar, CaO, and $CaCO_3$) was compared to the mass of the sample for the TG analysis and the volume of absorbed CO_2 during the gasification experiment was calculated. Characteristic temperatures based on TGA curves were determined: T_{in} is the initial decomposition temperature (when the decomposition rate increased to above 1%/min), T_{fin} is the temperature at which decomposition ended (when the decomposition rate decreased to below 1%/min), and T_{max} is the temperature at which the highest decomposition rate occurred. Detailed values can be found in Table 3 (together with the maximum decomposition rate (DTG_1)). The decomposition of $CaCO_3$ occurred between 650 and 800 °C. The gasification temperature of 800 °C, examined in the 6th test (N_2:CO_2, 1:1), was too high for CaO to absorb CO_2. The visible peak at 402 °C may originate from the decomposition of $Ca(OH)_2$. The calculated volume of absorbed CO_2 is presented in Table 2. The percentage value was determined in reference to the volume of carbon dioxide supplied with the gasifying atmosphere.

For N_2:CO_2 ratios of 1:1, 2:1, and 1:2, the total amount of supplied CO_2 was 1200 mL (1st and 3rd tests), 800 mL (4th test), and 1600 mL (5th test), respectively. A decrease in the CO_2 flow rate allowed for the higher absorption of CO_2 by CaO (58.7%), whereas the increase in the amount of supplied CO_2 caused the opposite effect (36.2%). Higher gasification temperature allowed for higher absorption of carbon dioxide when using the same N_2:CO_2 ratio: 615.2 ml (51.3%) at 700 °C compared to 490.4 ml (40.9%) at 600 °C. The stoichiometric reaction (5) reveals that efficiency of CO_2

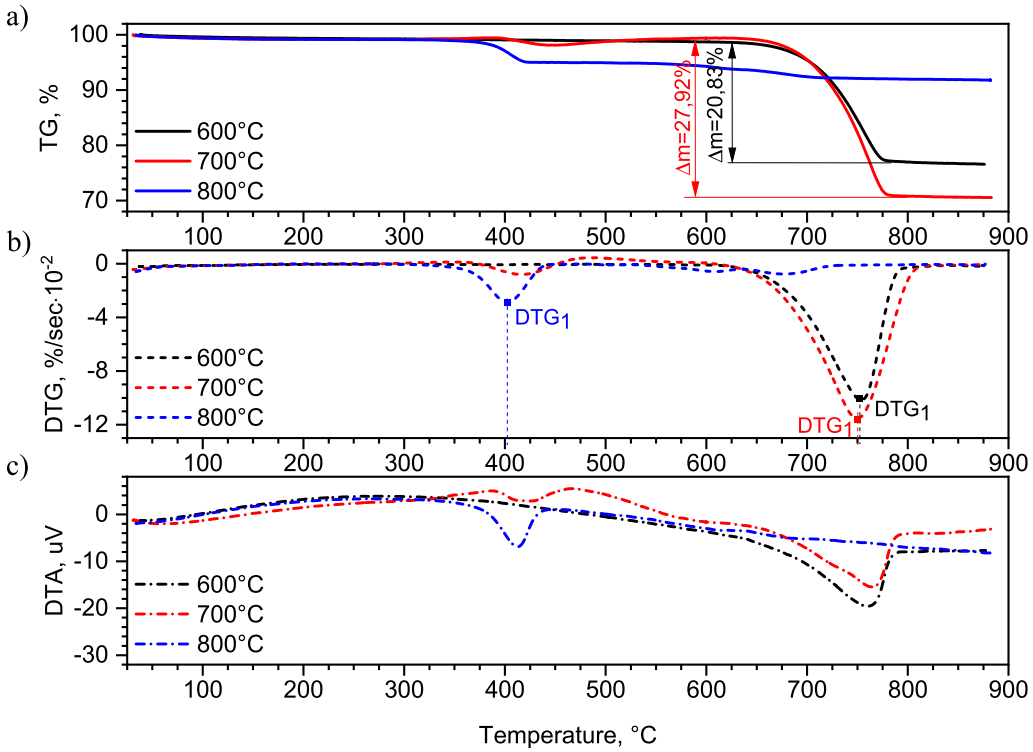

Fig. 2. TG (a), DTG (b), and DTA (c) curves received for samples after the gasification of PSD with CaO with a 50% concentration of CO_2 in the gasifying atmosphere at different temperatures.

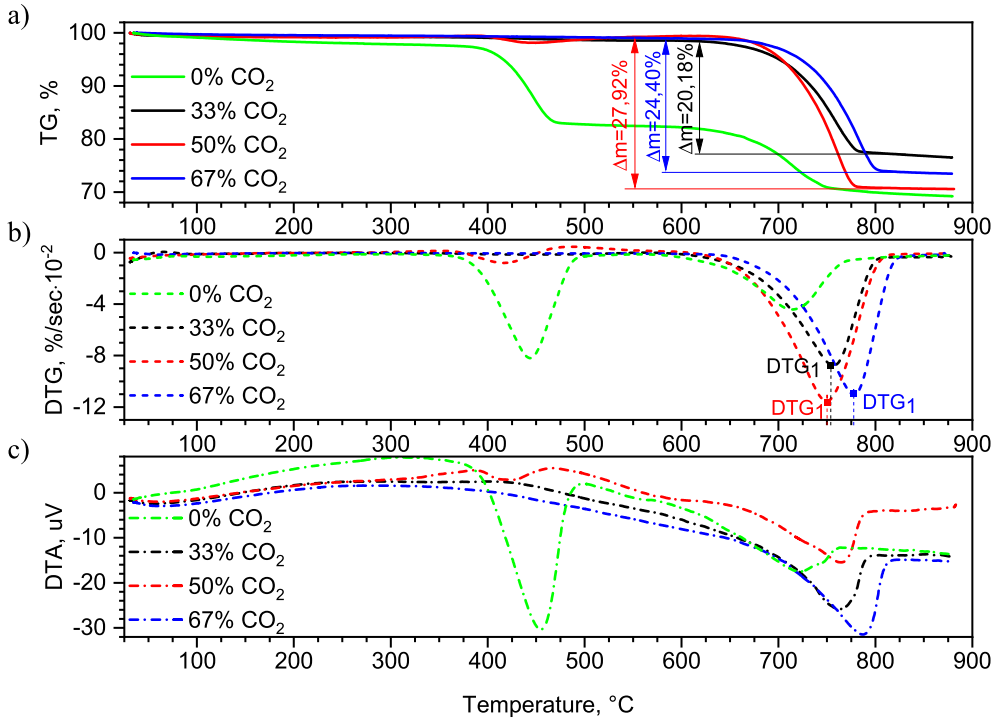

Fig. 3. TG (a), DTG (b), and DTA (c) curves received for samples after the gasification of PSD with CaO at 700 °C with different CO_2 concentration in the gasifying atmosphere.

Table 2
Volume of CO_2 absorbed by CaO during gasification experiments.

Test number	1	3	4	5
Gasification temperature, °C	600	700	700	700
Absorbed CO_2, ml	490.4	615.2	469.4	579.5
Absorbed CO_2, %	40.9	51.3	58.7	36.2
Concentration of CO_2 in gasifying atmosphere, %	50	50	33	67

Table 3
Characteristic temperatures based on thermogravimetric analysis.

Test number	1	3	4	5	6
Gasification temperature, °C	600	700	700	700	800
CO_2 concentration, %	50	50	33	67	50
T_{in}, °C	673	665	673	690	383
T_{fin}, °C	783	797	792	813	420
DTG_1, %/sec·10^{-2}	−10.17	−11.53	−8.78	−11.05	−2.89
T_{max}, °C	754	750	756	778	402

absorption ranges from 39 to 51%. The carbonation reaction is exothermic and supplies additional energy for the gasification process, thus increasing the overall energy efficiency of the process [50].

The test with 0% CO_2 concentration in the supplied atmosphere was used as a reference. Fig. 3 shows that decomposition of the residue started at approximately 400 °C (perhaps the decomposition of $Ca(OH)_2$). Second, the lower peak on the DTG curve indicates that the amount of absorbed CO_2 was much smaller.

3.3. Gas chromatography analysis

Gas analyses were conducted off-line with reference to the standard gas. Hydrogen (H_2), carbon monoxide (CO), methane (CH_4), carbon dioxide (CO_2), and nitrogen (N_2) were detected. The average values are presented in Figs. 4–6. Moreover, ethylene (C_2H_4), ethane (C_2H_6), propene (C_3H_6), and propane (C_3H_8) were also distinguished, but the negligible amounts were thus presented as C_XH_Y. The total amount of collected gases was achieved based on known nitrogen volume (flow rate and time) and the respective peak area chromatogram. The volume of other components was calculated by comparing the peak areas with reference to nitrogen. The results are presented in Table 4. Values received from the test at 700 °C with CaO and 50% of CO_2 (882.9 mL of syngas was collected during the heating stage, for 20 min between 300 and 700 °C, and 2077.1 ml of syngas were collected in final conditions, at 700 °C for 20 min) were set as reference points with a value of 100%.

During the gasification tests, $CO_2$was absorbed by calcium oxide. For reference, one run was conducted without the addition of CaO (2nd test) and one without CO_2 in the gasifying atmosphere (0^{th} test). The amount and composition of the produced gas were very different (Fig. 4). The experiment without CaO resulted in a higher concentration of carbon dioxide. Moreover, a very small amount of hydrogen was produced compared to other conditions, indicating the catalytic properties of CaO [55]. Removing CO_2 from the supplied atmosphere allowed us to observe different results. Based on the TGA results presented above, we conclude that part of the CaO was deactivated by transformation to $Ca(OH)_2$ [8], which may explain the high concentration of CO_2 in the second bag from test 0^{th} (Fig. 6). Furthermore, two aspects were investigated; the first was the temperature of gasification with a constant N_2:CO_2 ratio in the supplied atmosphere. The second study examined the influence of different CO_2 concentrations with a fixed temperature of 700 °C during gasification. Results from tests for a 1:1 N_2:CO_2 ratio presented an increase in the amount of syngas created by increasing the temperature (1st, 3rd, and 6th tests). Gasification at 600, 700, and 800 °C, generated a total of 2551.7, 2960, and 4772.2 mL of syngas, respectively, representing increases of 16% and 87% with respect to results at 600 °C. A lower concentration of carbon dioxide caused almost all of the CO_2 to be absorbed in the heating up stage

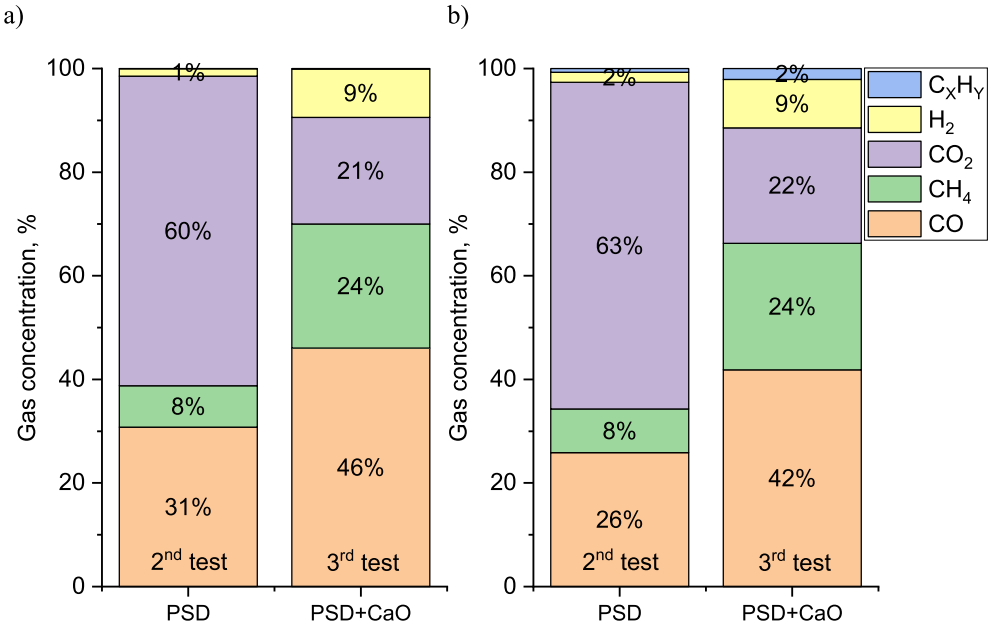

Fig. 4. Gas composition produced in the a) heating up stage and b) final conditions during gasification at 700 °C with 50% CO_2 concentration in gasifying atmosphere samples with and without CaO.

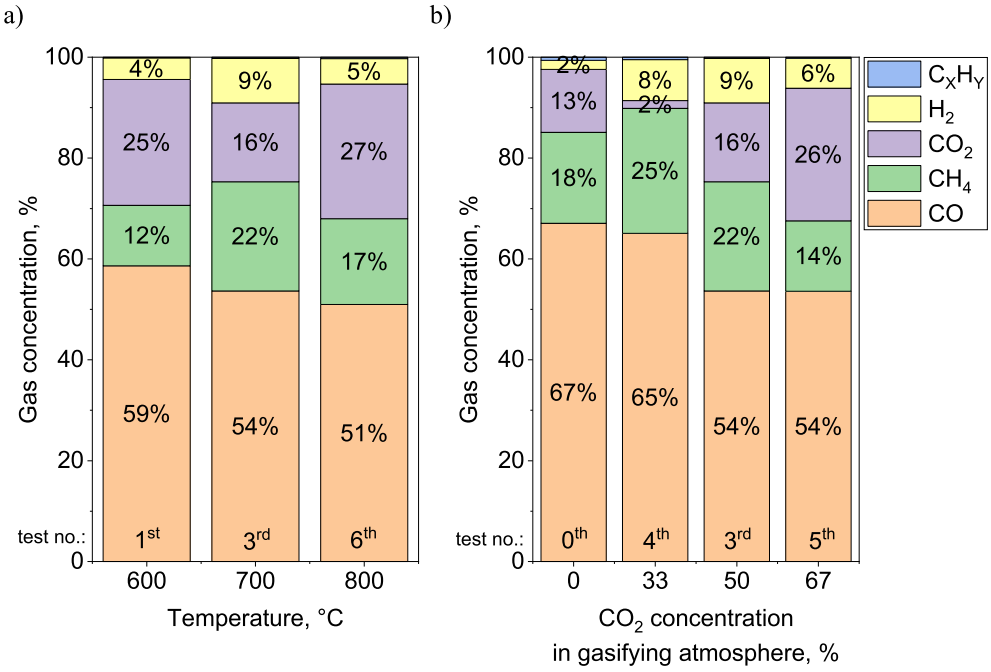

Fig. 5. Gas composition produced in the heating up stage) at different temperatures. b) with different CO_2 concentration in gasifying atmosphere.

(4th test). An increase in the CO_2 content in the gasifying atmosphere allowed for more CO_2 absorption in CaO, hence lowering the gas yield in the 5th test. The concentration of CO_2 in the syngas was directly related to the CO_2 concentration in the supplied atmosphere (Fig. 5b). Opposite correlation can be distinguished for CH_4 concentration, which decreases with increasing supplied CO_2 in the gasifying atmosphere.

All these trends were also visible in the gases collected during the final conditions (Fig. 6). Based on the temperature of gasification in this setup, 700 °C was chosen as the best option, because the concentration of CO_2 was much lower than at 600 °C, and more CH_4 and H_2 was produced than at 800 °C. During the test with a 1:2 N_2 to CO_2 ratio, the smallest amount of gas was produced, but the concentration of carbon dioxide had the smallest value. This could be connected to reaction (5) and the Boudouard reaction (6):

$$\boldsymbol{C + CO_2 \rightarrow 2CO} - 162.4\boldsymbol{kJ/mol} \quad (6)$$

Further collection of gas in the test at 800 °C resulted in a mixture of CO and CO_2. The amount of detected CO_2 originated primarily from the gasification atmosphere and decarbonation reaction of $CaCO_3$.

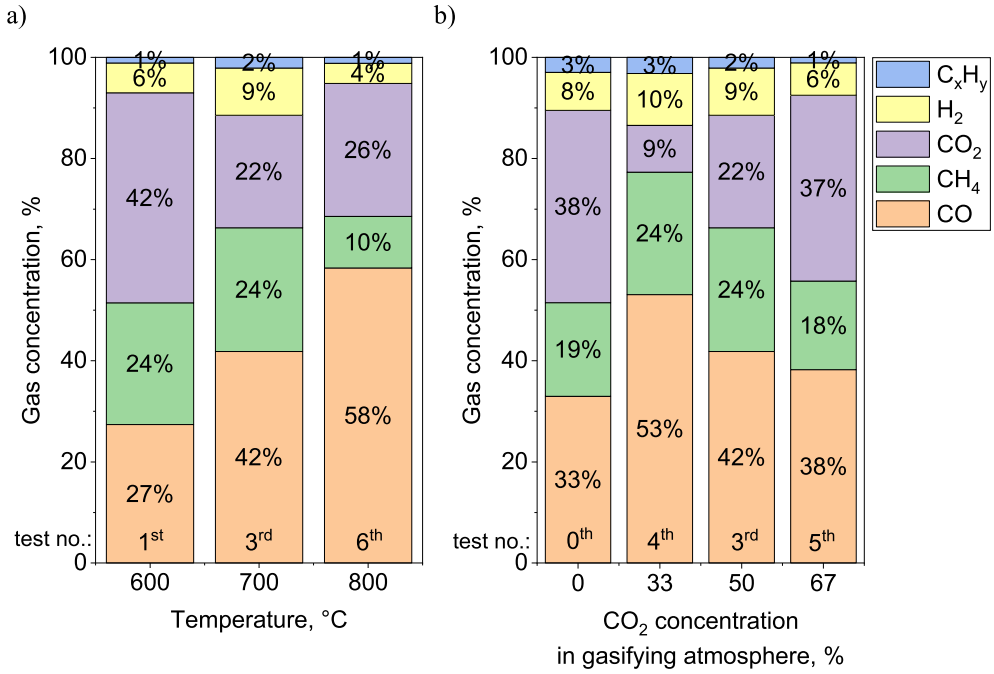

Fig. 6. Gas composition produced in the final stage a) at different temperatures. b) with different CO_2 concentrations in a gasifying atmosphere.

Table 4
Calculated volume of collected gases (without N_2).

Test number	0	1	2	3	4	5	6
Gasification temperature, °C	700	600	700	700	700	700	800
Heating up stage, %	135.2	67.4	177.5	100	85.2	65.7	112.4
Final conditions, %	58.7	94.2	149.5	100	68.2	115.2	182.0

Other investigators report the catalytic influence of CaO during gasification, which is conducted in a typical atmosphere of O_2/N_2 or H_2O/N_2. The addition of calcium oxide to these conditions enhances H_2 production. Wang et al. achieved a 44% hydrogen yield and simultaneous decrease in tar yield [56]. Similarly, Dong et al. reported a H_2 yield of up to 50% [57]. Both papers report decreased CO_2 concentration with increasing CaO input; however, gasification in a carbon dioxide atmosphere changes the composition of the received gas. Sun et al. proposed new 'Auto-CaL-Gas' technology, which CO_2 gasification is connected with autothermal CaO looping [50]. Their experiment, conducted at 650 °C, produced results comparable to those presented in this paper. The effects of CaO addition and CO_2 concentration are confirmed. Here, we present an additional aspect of the temperature influence and different ratios of N_2 to CO_2. Baranowski et al. studied gasification of refuse-derived fuel mixed with sewage sludge in a CO_2 atmosphere with the addition of CaO and reported that (similar to Fig. 4) calcium oxide increased concentrations of CO and CH_4—which were assigned to the catalytic properties of CaO [55].

3.4. Fourier-transform infrared spectroscopy analysis

Fourier-transform infrared spectroscopy was conducted to investigate gases released during thermogravimetric analysis in a nitrogen atmosphere of the sample obtained from the test conducted at 700 °C with a 1:1 N_2:CO_2 ratio and a mixture of PSD and CaO. Results are presented in Figs. 7–9 and Table 5.

Based on the mass loss (TG curves) and its derivative (DTG curves), specific temperatures were chosen to investigate the FTIR

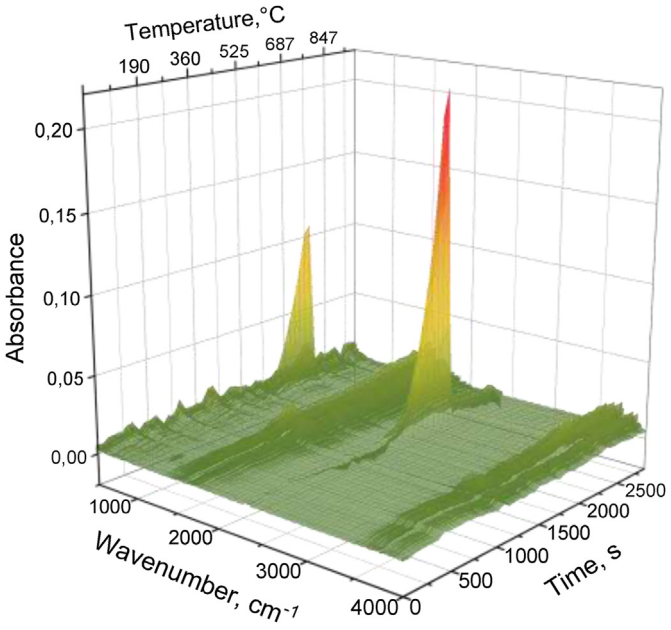

Fig. 7. TG-FTIR spectra of residue from the test 700 °C, PSD + CaO, N_2:CO_2 1:1.

spectra. At temperatures of 386, 425, and 445 °C, only broad bands in the range 1300–1800 cm^{-1} and 3500–4000 cm^{-1} can be distinguished. The occurrence suggests the presence of gaseous water. At higher temperatures (642, 756, and 777 °C), strong peaks appeared at approximately 2250–2350 cm^{-1} and 669 cm^{-1} that were associated with the release of CO_2. Additionally, a low peak was observed at approximately 2100–2200 cm^{-1}, revealing traces of carbon oxide [58,59]. TG-FTIR analysis confirmed that mass loss above 600 °C is connected to the decarbonation reaction of $CaCO_3$. Similar conclusions were reached by Ding et al. studying in-situ CO_2 capture using a CaO catalyst during herb residue analysis [60].

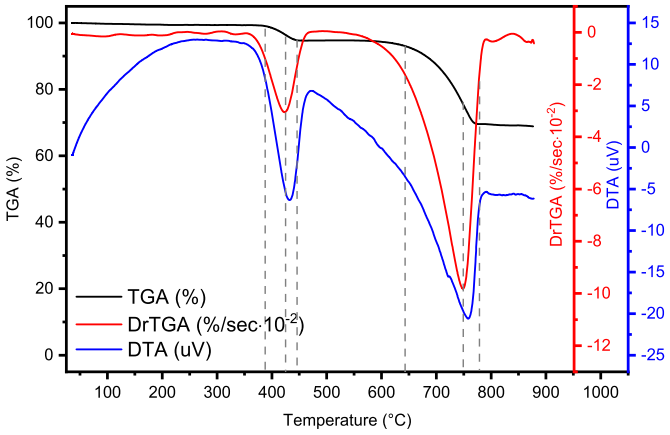

Fig. 8. TG, DTG, and DTA curves from analysis conducted in N_2 atmosphere of residue from the test 700 °C, PSD + CaO, N_2:CO_2 1:1.

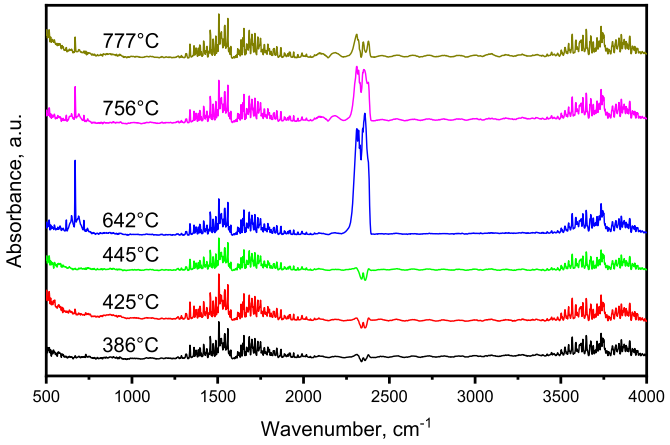

Fig. 9. FTIR spectra-derived for specific temperatures based on TG and DTG curves.

Table 5
Characteristic bands, their vibration and assigned compounds.

Wavenumber, cm^{-1}	Vibration	Compound
669	-	CO_2
1300–1800	O–H stretch	H_2O
2100–2200	-	CO
2250–2400	-	CO_2
3500–4000	O–H stretch	H_2O

Table 6
Calculated high heating value of received gases.

Test number	1	2	3	4	5	6
Gasification temperature, °C	600	700	700	700	700	800
Heating up stage, MJ/m^3	12.74	7.95	16.63	19.37	13.16	13.94
Final conditions, MJ/m^3	14.52	7.34	17.61	19.74	13.32	12.69

3.5. High heating value determination

Calculated HHVs of received gases are presented in Table 6.

The highest energy potential is assigned to gas from the test with the lowest CO_2 flow rate during the gasification process and is connected to a high content of carbon oxide, methane, and hydrogen and a relatively low carbon dioxide concentration. The investigated gases were purged from water vapour, and thus their low and high heating values were equal. For comparison, the LHV of a 1:1 H_2:CO mixture is 11.65 MJ/m^3 [61].

3.6. Syngas production

The most important aspect of syngas production is the concentration of hydrogen and carbon monoxide in the received gas. The mixture of these two gases is a desirable product of the thermal conversion of solid feedstock, especially in gasification. CO and H_2 can be released directly from broken molecules of biomass but are also produced by reactions between char and gasification agents. In this study, carbon dioxide was used as the gasification agent, and the Boduard reaction (6) creates more carbon monoxide. Additionally, calcium oxide can be used to absorb carbon dioxide (5), the Boduard reaction can be stopped, and a lower concentration of carbon monoxide is observed. Fig. 10 shows the cumulative concentration of collected gases, especially carbon monoxide and hydrogen, during the gasification tests.

A small amount of hydrogen was generated in all cases. The highest concentrations of hydrogen and carbon monoxide were detected at 700 °C for a 2:1 ratio of N_2:CO_2 (4th test). The smallest amount of hydrogen and carbon monoxide was observed for the test at 700 °C and a 1:1 ratio of N_2:CO_2 without CaO addition (2nd test). The addition of calcium oxide to the biomass sample increased syngas production.

4. Conclusions

The impacts of process temperature, the presence of calcium oxide, and the concentration of carbon dioxide in the gasifying atmosphere during biomass gasification were determined. A temperature of 800 °C did not allow for the carbonation reaction of CaO. The presence of CaO allowed for CO_2 absorption and decreased the overall production of CO_2. The addition of CaO also helped increase hydrogen production (up to 10% concentration) and significantly improved the LHV of the received syngas. The most interesting results were received at 700 °C with flow rates of 40 ml/min N_2 and 20 ml/min CO_2 for a mixture of pine sawdust with CaO. The amount of supplied carbon dioxide reached 800 ml during 40 min of experiments, whereas the collected gas contained 143 ml (17.9%) of CO_2—based on calculations, 469.4 ml (58.7%) of CO_2 were bonded in calcium carbonate, suggesting that 187.6 mL (23.4%) of CO_2 was utilised during the process. This topic needs to be further investigated to propose a process that provides a possible solution

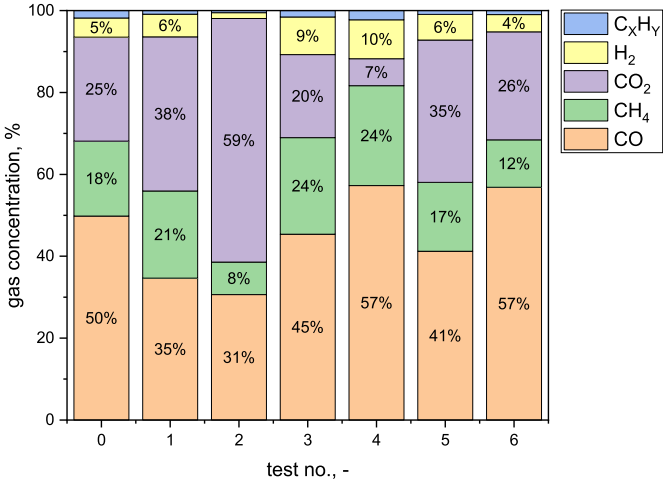

Fig. 10. Cumulative gas composition from gasification tests.

for decreasing carbon dioxide pollution in the atmosphere while creating usable products. This produced gas could be further utilised during proper syngas production.

Declaration of competing interest

The authors declare that they have no known competing financial interests or personal relationships that could have appeared to influence the work reported in this paper.

Acknowledgment

This project has received funding from the European Union's Horizon 2020 research and innovation programme under the Marie Skłodowska-Curie grant agreement No 823745. The Key Program for China-EU International Cooperation in Science and Technology Innovation (No. 2018YFE0117300), Shaanxi Provincial Natural Science Foundation Research Program-Shaanxi Coal Joint Funding (2019JLZ-12). Many thanks to the technicians in Analytical and Testing Center of Xi'a Jiaotong University.

References

[1] International Energy Agency, Key World Energy Statistics, 2009.
[2] International Energy Agency, Key World Energy Statistics, 2019.
[3] G.P. Peters, R.M. Andrew, S. Solomon, P. Friedlingstein, Measuring a fair and ambitious climate agreement using cumulative emissions, Environ. Res. Lett. 10 (2015) 105004, https://doi.org/10.1088/1748-9326/10/10/105004.
[4] J.H. Williams, A. DeBenedictis, R. Ghanadan, A. Mahone, J. Moore, W.R. Morrow III, S. Price, M.S. Torn, The technology path to deep greenhouse gas emissions cuts by 2050: the pivotal role of electricity, Science 335 (2012) 53–59, https://doi.org/10.1126/science.1208365.
[5] K. Bulkowska, Z.M. Gusiatin, E. Klimiuk, A. Pawłowski, T. Pokój, Biomass for Biofuels, CRC Press, 2016, https://doi.org/10.1201/9781315226422.
[6] P. Basu, Biomass Gasification, Pyrolysis and Torrefaction: Practical Design and Theory, second ed., Elsevier, London, 2013 https://doi.org/10.1016/C2011-0-07564-6.
[7] S. Szwaja, A. Magdziarz, M. Zajemska, A. Poskart, A torrefaction of Sida hermaphrodita to improve fuel properties. Advanced analysis of torrefied products, Renew. Energy 141 (2019) 894–902, https://doi.org/10.1016/j.renene.2019.04.055.
[8] M. Sieradzka, N. Gao, C. Quan, A. Mlonka-Mędrala, A. Magdziarz, Biomass thermochemical conversion via pyrolysis with integrated CO $_2$ capture, Energies 13 (2020) 1050, https://doi.org/10.3390/en13051050.
[9] M. Wilk, A. Magdziarz, I. Kalemba-Rec, M. Szymańska-Chargot, Upgrading of green waste into carbon-rich solid biofuel by hydrothermal carbonization: the effect of process parameters on hydrochar derived from acacia, Energy (2020) 117717, https://doi.org/10.1016/j.energy.2020.117717.
[10] N. Gao, K. Kamran, C. Quan, P.T. Williams, Thermochemical conversion of sewage sludge: a critical review, Prog. Energy Combust. Sci. 79 (2020) 100843, https://doi.org/10.1016/j.pecs.2020.100843.
[11] M. Śliz, M. Wilk, A comprehensive investigation of hydrothermal carbonization: energy potential of hydrochar derived from Virginia mallow, Renew. Energy (2020), https://doi.org/10.1016/j.renene.2020.04.124.
[12] Y. Chai, M. Wang, N. Gao, Y. Duan, J. Li, Experimental study on pyrolysis/gasification of biomass and plastics for H2 production under new dual-support catalyst, Chem. Eng. J. 396 (2020) 125260, https://doi.org/10.1016/j.cej.2020.125260.
[13] A.S. Al-Rahbi, J.A. Onwudili, P.T. Williams, Thermal decomposition and gasification of biomass pyrolysis gases using a hot bed of waste derived pyrolysis char, Bioresour. Technol. 204 (2016) 71–79, https://doi.org/10.1016/j.biortech.2015.12.016.
[14] N. Ramzan, A. Ashraf, S. Naveed, A. Malik, Simulation of hybrid biomass gasification using Aspen plus: a comparative performance analysis for food, municipal solid and poultry waste, Biomass Bioenergy 35 (2011) 3962–3969, https://doi.org/10.1016/j.biombioe.2011.06.005.
[15] W. Doherty, A. Reynolds, D. Kennedy, The effect of air preheating in a biomass CFB gasifier using ASPEN Plus simulation, Biomass Bioenergy 33 (2009) 1158–1167, https://doi.org/10.1016/j.biombioe.2009.05.004.
[16] X.T. Li, J.R. Grace, C.J. Lim, A.P. Watkinson, H.P. Chen, J.R. Kim, Biomass gasification in a circulating fluidized bed, Biomass Bioenergy 26 (2004) 171–193, https://doi.org/10.1016/S0961-9534(03)00084-9.
[17] J. Han, H. Kim, The reduction and control technology of tar during biomass gasification/pyrolysis: an overview, Renew. Sustain. Energy Rev. 12 (2008) 397–416, https://doi.org/10.1016/j.rser.2006.07.015.
[18] J. Zhang, P. Jiang, F. Gao, Z. Ren, R. Li, H. Chen, X. Ma, Q. Hao, Fuel gas production and char upgrading by catalytic CO2 gasification of pine sawdust char, Fuel 280 (2020) 118686, https://doi.org/10.1016/j.fuel.2020.118686.
[19] M. Karaca, D. Kaya, A. Yozgatligil, I. Gökalp, Modeling and numerical simulations of lignite char gasification with CO2: the effect of gasification parameters on internal transport phenomena, Fuel 285 (2021), https://doi.org/10.1016/j.fuel.2020.119067, 119067.
[20] S. Cheah, W.S. Jablonski, J.L. Olstad, D.L. Carpenter, K.D. Barthelemy, D.J. Robichaud, J.C. Andrews, S.K. Black, M.D. Oddo, T.L. Westover, Effects of thermal pretreatment and catalyst on biomass gasification efficiency and syngas composition, Green Chem. 18 (2016) 6291–6304, https://doi.org/10.1039/C6GC01661H.
[21] D.W. Cho, D.C.W. Tsang, S. Kim, E.E. Kwon, G. Kwon, H. Song, Thermochemical conversion of cobalt-loaded spent coffee grounds for production of energy resource and environmental catalyst, Bioresour. Technol. 270 (2018) 346–351, https://doi.org/10.1016/j.biortech.2018.09.046.
[22] L. Tang, Y. Yan, Y. Meng, J. Wang, P. Jiang, C.H. Pang, T. Wu, CO2 gasification and pyrolysis reactivity evaluation of oil shale, Energy Procedia 158 (2019) 1694–1699, https://doi.org/10.1016/j.egypro.2019.01.394.
[23] C. Breidenich, D. Magraw, A. Rowley, J.W. Rubin, The kyoto protocol to the united Nations Framework convention on climate change, Am. J. Int. Law 92 (1998) 315–331, https://doi.org/10.2307/2998044.
[24] European Commission, Communication from the Commission to the European Parliament, the Council, the European Economic and Social Committee and the Committee of the Regions - 20 20 by 2020 - Europe's Climate Change Opportunity, COM 30 Final, 2008. Brussels.
[25] C. Dinca, N. Slavu, C.C. Cormoş, A. Badea, CO2 capture from syngas generated by a biomass gasification power plant with chemical absorption process, Energy 149 (2018) 925–936, https://doi.org/10.1016/j.energy.2018.02.109.
[26] J. Zhang, M. Ren, X. Li, Y. Ge, F. Gao, H. Chen, Q. Hao, X. Ma, Syngas production by integrating CO2 partial gasification of pine sawdust and methane pyrolysis over the gasification residue, Int. J. Hydrogen Energy 44 (2019) 19742–19754, https://doi.org/10.1016/j.ijhydene.2019.06.014.
[27] M.H. Doranehgard, H. Samadyar, M. Mesbah, P. Haratipour, S. Samiezade, High-purity hydrogen production with in situ CO2 capture based on biomass gasification, Fuel 202 (2017) 29–35, https://doi.org/10.1016/j.fuel.2017.04.014.
[28] M. Perander, N. DeMartini, A. Brink, J. Kramb, O. Karlström, J. Hemming, A. Moilanen, J. Konttinen, M. Hupa, Catalytic effect of Ca and K on CO2 gasification of spruce wood char, Fuel 150 (2015) 464–472, https://doi.org/10.1016/j.fuel.2015.02.062.
[29] M. Jeremiáš, M. Pohořelý, K. Svoboda, V. Manovic, E.J. Anthony, S. Skoblia, Z. Beňo, M. Šyc, Gasification of biomass with CO2 and H2O mixtures in a catalytic fluidised bed, Fuel 210 (2017) 605–610, https://doi.org/10.1016/j.fuel.2017.09.006.
[30] B. Hejazi, J.R. Grace, X. Bi, A. Mahecha-Botero, Steam gasification of biomass coupled with lime-based CO2 capture in a dual fluidized bed reactor: a modeling study, Fuel 117 (2014) 1256–1266, https://doi.org/10.1016/j.fuel.2013.07.083.
[31] H. Liu, B.M. Gibbs, Modeling NH3 and HCN emissions from biomass circulating fluidized bed gasifiers, Fuel 82 (2003) 1591–1604, https://doi.org/10.1016/S0016-2361(03)00091-7.
[32] B.R. Strazisar, R.R. Anderson, C.M. White, Degradation pathways for monoethanolamine in a CO2 capture facility, Energy Fuel. 17 (2003) 1034–1039, https://doi.org/10.1021/ef020272i.
[33] E. Mostafavi, N. Mahinpey, M. Rahman, M.H. Sedghkerdar, R. Gupta, High-purity hydrogen production from ash-free coal by catalytic steam gasification integrated with dry-sorption CO2 capture, Fuel 178 (2016) 272–282, https://doi.org/10.1016/j.fuel.2016.03.026.
[34] S. Chen, D. Wang, Z. Xue, X. Sun, W. Xiang, Calcium looping gasification for high-concentration hydrogen production with CO2 capture in a novel compact fluidized bed: simulation and operation requirements, Int. J. Hydrogen Energy 36 (2011) 4887–4899, https://doi.org/10.1016/j.ijhydene.2010.12.130.
[35] N. Gao, K. Chen, C. Quan, Development of CaO-based adsorbents loaded on charcoal for CO2 capture at high temperature, Fuel 260 (2020) 116411, https://doi.org/10.1016/j.fuel.2019.116411.
[36] N.H. Florin, A.T. Harris, Hydrogen production from biomass coupled with carbon dioxide capture: the implications of thermodynamic equilibrium, Int. J. Hydrogen Energy 32 (2007) 4119–4134, https://doi.org/10.1016/j.ijhydene.2007.06.016.
[37] B. Acharya, A. Dutta, P. Basu, An investigation into steam gasification of biomass for hydrogen enriched gas production in presence of CaO, Int. J. Hydrogen Energy 35 (2010) 1582–1589, https://doi.org/10.1016/j.ijhydene.2009.11.109.
[38] Z. Wang, J. Zhou, Q. Wang, J. Fan, K. Cen, Thermodynamic equilibrium analysis of hydrogen production by coal based on Coal/CaO/H2O gasification system, Int. J. Hydrogen Energy 31 (2006) 945–952, https://doi.org/10.1016/j.ijhydene.2005.07.010.
[39] A. Di Giuliano, J. Girr, R. Massacesi, K. Gallucci, C. Courson, Sorption enhanced steam methane reforming by Ni–CaO materials supported on mayenite, Int. J. Hydrogen Energy 42 (2017) 13661–13680, https://doi.org/10.1016/j.ijhydene.2016.11.198.
[40] M.R. Cesário, B.S. Barros, C. Courson, D.M.A. Melo, A. Kiennemann, Catalytic performances of Ni-CaO-mayenite in CO2 sorption enhanced steam methane reforming, Fuel Process. Technol. 131 (2015) 247–253, https://doi.org/10.1016/j.fuproc.2014.11.028.
[41] Q. Hu, Y. Shen, J.W. Chew, T. Ge, C.H. Wang, Chemical looping gasification of

biomass with Fe2O3/CaO as the oxygen carrier for hydrogen-enriched syngas production, Chem. Eng. J. 379 (2020) 122346, https://doi.org/10.1016/j.cej.2019.122346.
[42] Y. Wu, Y. Liao, G. Liu, X. Ma, Syngas production by chemical looping gasification of biomass with steam and CaO additive, Int. J. Hydrogen Energy 43 (2018) 19375–19383, https://doi.org/10.1016/j.ijhydene.2018.08.197.
[43] Q. Liu, C. Hu, B. Peng, C. Liu, Z. Li, K. Wu, H. Zhang, R. Xiao, High H2/CO ratio syngas production from chemical looping co-gasification of biomass and polyethylene with CaO/Fe2O3 oxygen carrier, Energy Convers. Manag. 199 (2019) 111951, https://doi.org/10.1016/j.enconman.2019.111951.
[44] C.T. Performance, A review of phosphorus removal structures: how to assess and compare their performance. https://doi.org/10.3390/w9080583, 2017, 1-22.
[45] J. Udomsirichakorn, P.A. Salam, Review of hydrogen-enriched gas production from steam gasification of biomass: the prospect of CaO-based chemical looping gasification, Renew. Sustain. Energy Rev. 30 (2014) 565–579, https://doi.org/10.1016/j.rser.2013.10.013.
[46] J. Udomsirichakorn, P. Basu, P. Abdul Salam, B. Acharya, CaO-based chemical looping gasification of biomass for hydrogen-enriched gas production with in situ CO2 capture and tar reduction, Fuel Process. Technol. 127 (2014) 7–12, https://doi.org/10.1016/j.fuproc.2014.06.007.
[47] H. Nam, S. Wang, K.C. Sanjeev, M.W. Seo, S. Adhikari, R. Shakya, D. Lee, S.R. Shanmugam, Enriched hydrogen production over air and air-steam fluidized bed gasification in a bubbling fluidized bed reactor with CaO: effects of biomass and bed material catalyst, Energy Convers. Manag. 225 (2020) 113408, https://doi.org/10.1016/j.enconman.2020.113408.
[48] R.Y. Chein, W.H. Hsu, Thermodynamic equilibrium analysis of H2-rich syngas production via sorption-enhanced chemical looping biomass gasification, Renew. Energy 153 (2020) 117–129, https://doi.org/10.1016/j.renene.2019.10.097.
[49] S. Zhang, N. Gao, C. Quan, F. Wang, C. Wu, Autothermal CaO looping biomass gasification to increase process energy efficiency and reduce ash sintering, Fuel 277 (2020), https://doi.org/10.1016/j.fuel.2020.118199.
[50] H. Sun, C. Wu, Autothermal CaO looping biomass gasification for renewable syngas production, Environ. Sci. Technol. 53 (2019) 9298–9305, https://doi.org/10.1021/acs.est.9b01527.
[51] Y. Cengel, M. Boles, Appendix 1; table A-27, in: Thermodyn. - an Eng. Approach, eighth ed., McGraw-Hill, 2015, p. 939.
[52] L. Han, Q. Wang, Z. Luo, N. Rong, G. Deng, H2 rich gas production via pressurized fluidized bed gasification of sawdust with in situ CO2 capture, Appl. Energy 109 (2013) 36–43, https://doi.org/10.1016/j.apenergy.2013.03.035.
[53] S. Lin, M. Harada, Y. Suzuki, H. Hatano, Continuous experiment regarding hydrogen production by Coal/CaO reaction with steam (II) solid formation, Fuel 85 (2006) 1143–1150, https://doi.org/10.1016/j.fuel.2005.05.029.
[54] X. Zhou, J. Zhao, S. Guo, J.J. Li, Z. Yu, S.S. Song, J.J. Li, Y. Fang, High quality syngas production from pressurized K2CO3 catalytic coal gasification with in-situ CO2 capture, Int. J. Hydrogen Energy 43 (2018) 17091–17099, https://doi.org/10.1016/j.ijhydene.2018.07.062.
[55] M. Baranowski, M. Frydel, H. Pawlak-Kruczek, Effect of gasifying agents and calcium oxide on gasification of low-rank coal and wastes, Trans. Institue Fluid-Flow Mach. 137 (2017) 141–155.
[56] M. Wang, Y. Qi, R. Ma, Z. Fu, P. Ge, S. Ji, J. Wu, X. Qian, Investigation of CaO influences on fast gasification characteristics of biomass in a fixed-bed reactor, Waste and Biomass Valorization (2019) 1–8, https://doi.org/10.1007/s12649-019-00694-x.
[57] J. Dong, A. Nzihou, Y. Chi, E. Weiss-Hortala, M. Ni, N. Lyczko, Y. Tang, M. Ducousso, Hydrogen-Rich gas production from steam gasification of biochar in the presence of CaO, Waste and Biomass Valorization 8 (2017) 2735–2746, https://doi.org/10.1007/s12649-016-9784-x.
[58] N. Gao, A. Li, C. Quan, L. Du, Y. Duan, TG-FTIR and Py-GC/MS analysis on pyrolysis and combustion of pine sawdust, J. Anal. Appl. Pyrolysis 100 (2013) 26–32, https://doi.org/10.1016/j.jaap.2012.11.009.
[59] K. Coenen, F. Gallucci, B. Mezari, E. Hensen, M. van Sint Annaland, An in-situ IR study on the adsorption of CO2 and H2O on hydrotalcites, J. CO2 Util. 24 (2018) 228–239, https://doi.org/10.1016/j.jcou.2018.01.008.
[60] W. Ding, X. Zhang, B. Zhao, W. Zhou, A. Xu, L. Chen, L. Sun, S. Yang, H. Guan, X. Xie, G. Chen, L. Zhu, G. Song, TG-FTIR and thermodynamic analysis of the herb residue pyrolysis with in-situ CO 2 capture using CaO catalyst, J. Anal. Appl. Pyrolysis 134 (2018) 389–394, https://doi.org/10.1016/j.jaap.2018.07.005.
[61] F.Y. Hagos, A.R.A. Aziz, S.A. Sulaiman, B.K.M. Mahgoub, Low and medium calorific value gasification gas combustion in IC engines, in: K.G. Kyprianidis, J. Skvaril (Eds.), Dev. Combust. Technol., 2016, https://doi.org/10.5772/64459.